Room-temperature growth of Mg on Si(111): stepwise versus continuous deposition

2007 J. Phys.: Condens. Matter 19 266004

(http://iopscience.iop.org/0953-8984/19/26/266004)

IOP PUBLISHING JOURNAL OF PHYSICS: CONDENSED MATTER

J. Phys.: Condens. Matter **19** (2007) 266004 (10pp) doi:10.1088/0953-8984/19/26/266004

Room-temperature growth of Mg on Si(111): stepwise versus continuous deposition

Dohyun Lee[1], Geunseop Lee[2], Sehun Kim[3], Chanyong Hwang[1], Ja-Yong Koo[1] and Hangil Lee[4]

[1] Advanced Industrial Technology Group, Division of Advanced Technology, Korea Research Institute of Standards and Science, Daejeon 305-600, Korea
[2] Department of Physics, Inha University, Inchon 402-751, Korea
[3] Department of Chemistry and School of Molecular Science (BK21), Korea Advanced Institute of Science and Technology, Daejeon 305-701, Korea
[4] Beamline Research Division, Pohang Accelerator Laboratory (PAL), POSTECH, Pohang, Kyongbuk 790-784, Korea

E-mail: easyscan@postech.ac.kr (H Lee)

Received 1 February 2007, in final form 16 April 2007
Published 31 May 2007
Online at stacks.iop.org/JPhysCM/19/266004

Abstract

Using low-energy electron diffraction and scanning tunnelling microscopy, we studied the formation of Mg silicide and metallic Mg islands on a Si(111)-7 × 7 surface at room temperature as a function of Mg coverage. We found that the mechanism by which Mg islands grew on the Si(111)-7 × 7 surface, and the morphology of the islands that formed, depended on whether the Mg deposition was performed in a stepwise or continuous manner. When Mg was deposited in a stepwise manner, with 1 h between deposition events, an amorphous Mg silicide overlayer formed on the Si(111)-7 × 7 surface during the initial stage of deposition (up to 2.0 ML Mg coverage), as shown by the observation of $\delta 7 \times 7$ and 1×1 low-energy electron diffraction patterns. Upon further stepwise Mg deposition, round-shaped Mg islands grew on the amorphous Mg silicide layer, as shown by scanning tunnelling microscopy and the emergence of a 1 × 1 low-energy electron diffraction pattern. If, on the other hand, the Mg was deposited continuously in a single step, hexagonal Mg islands formed on the flat Mg silicide layers, and a $(\frac{2}{3}\sqrt{3} \times \frac{2}{3}\sqrt{3})$R30° and 1 × 1 mixed phase was observed. Moreover, using scanning tunnelling spectroscopy, we confirmed the semiconducting and metallic nature of the Mg silicide layer and hexagonal Mg islands on the Si(111)-7 × 7 surface depending on their Mg coverage, respectively.

(Some figures in this article are in colour only in the electronic version)

1. Introduction

Over the past decades, the adsorption of alkali and alkaline earth metals onto semiconductor surfaces has been intensively studied not only from a pure science perspective but also due to the many technological applications involving these adsorption processes [1–7]. Several studies have examined the formation of Mg silicide and Mg-induced superstructures on the Si(111)-7 × 7 surface using a range of experimental techniques, including low-energy electron diffraction (LEED), photoemission spectroscopy (PES), and scanning tunnelling microscopy (STM). Vandre *et al* [8] observed that, as Mg atoms were adsorbed onto a Si(111)-7 × 7 surface at room temperature (RT), the 7 × 7 LEED patterns gradually disappeared and new $(\sqrt{3} \times \sqrt{3})$R30° (hereafter $\sqrt{3}$) patterns emerged. However, Quinn *et al* [9] suggested that the $\sqrt{3}$ and 3 × 3 patterns were actually misinterpretations of $(\frac{2}{3}\sqrt{3} \times \frac{2}{3}\sqrt{3})$R30° (hereafter $\frac{2}{3}\sqrt{3}$) and 3 × 1 patterns, respectively. Moreover, no LEED patterns were seen at very high Mg coverage. During slow Mg deposition at RT or at slightly elevated temperatures (100–200 °C), initially a 7 × 7 pattern is observed, which changes into a mixture of 1 × 1 and $\frac{2}{3}\sqrt{3}$ patterns as the Mg coverage increases, finally becoming a $\frac{2}{3}\sqrt{3}$ pattern at higher coverages [8]. Quinn *et al* [9] also suggested that these patterns are due to Mg_2Si silicide and that the Si reconstructed surface is stabilized by adsorbed metal atoms, which do not have long-range order on the basis of their LEED current–voltage (I–V) plot. Therefore, they excluded the possibility that the metal atoms are arranged periodically on the surface. Wirgen *et al* [10] confirmed the 3 × 1 and $\frac{2}{3}\sqrt{3}$ LEED patterns reported by Quinn *et al*. They showed that the relations between $\frac{2}{3}\sqrt{3}$ LEED patterns and atomic structural models are schematically shown in [10]. In addition, on the basis of PES results, they reported that Mg_2Si silicide is a semiconductor with an indirect band gap of 0.6 eV and a direct band gap of 2.17 eV. An *et al* studied the initial interface and silicide formation induced by Mg adsorption on a Si(111)-7 × 7 surface at RT using LEED and PES [11, 12]. Despite there being an STM study of Mg-induced 3 × 2 reconstructions on Si(111) surface at elevated substrate temperature [13], to our knowledge no systematic STM study has yet been carried out on the RT growth of Mg silicide on this surface.

In the present work, we used STM and LEED to study the adsorption of Mg onto a Si(111)-7 × 7 surface at various coverages and compared two mechanisms for the growth of a Mg silicide layer formed by the interaction between Mg atoms and the Si(111)-7 × 7 surface (stepwise deposition and continuous deposition). In addition, we investigated the metallic Mg island growth mode at higher Mg coverages. Furthermore, we determined the electronic properties of Mg silicide and Mg overlayers on a Si(111)-7×7 surface using scanning tunnelling spectroscopy (STS).

2. Experimental details

The experiments were performed in an ultrahigh-vacuum (UHV) chamber with a base pressure of 2.0×10^{-10} Torr, which was equipped with a home-made UHV scanning tunnelling microscope and Omicron LEED optics. An n-type Si(111) sample with a resistivity of 0.1 Ω cm was cut from a commercial Si wafer, cleaned by several cycles of heating to 1200 °C after outgassing at 600 °C for more than 12 h. The cleanliness of the Si(111)-7 × 7 surface was confirmed by examination of STM images and LEED patterns. To produce Mg adsorption for deposition onto the Si(111)-7 × 7 surface, Mg was evaporated by placing several Mg grains (99.99%) in a pyrolytic boron nitride (PBN) crucible coiled by W wire, which was then heated, causing the Mg grains to be heated indirectly. Prior to evaporation, the Mg grains were also degassed for 24 h. The Mg deposition flux was 0.1 monolayer (ML) min^{-1}, as calibrated by a quartz thickness monitor. All Mg deposition was performed at RT. STM, LEED, and Auger

electron spectroscopy (AES) were also used to check the purity of the Mg source and Si sample. In the AES spectrum of the Mg-adsorbed Si(111) surface, the only peaks observed were the Mg (48 eV) and Si (96 eV) ones. During the evaporation of Mg, the pressure of the UHV chamber was kept below 5.0×10^{-10} Torr. The scanning transmission microscope tip was prepared by cutting W wire (diameter 0.5 mm) followed by etching in a 0.1 N NaOH solution. The prepared tip was cleaned by electron bombardment in the UHV chamber. In the constant-current imaging mode at 0.1 nA, the sample bias voltage was set to +2.0 V.

3. Results and discussion

To clarify the discrepancy between the different growth patterns observed for the Mg silicide and Mg overlayer, we used STM, STS, and LEED to investigate the characteristics of the stepwise and continuous deposition processes.

Figure 1 shows empty-state STM images of Mg grown on a Si(111)-7 × 7 surface at coverages ranging from 0 to 6.0 ML by stepwise Mg deposition with a time interval of 1 h (multi-step deposition) at RT. After confirming that the original Si(111)-7 × 7 surface was clean (figure 1 (a)), we deposited 0.1 ML Mg on the Si(111)-7 × 7 surface (figure 1(b)). As shown in this image, the deposited Mg atoms are randomly adsorbed on the Si(111)-7 × 7 surface without any surface reconstruction. It is noted that the adsorbed Mg does not interact with the Si(111)-7 × 7 surface at this submonolayer coverage. However, when the coverage was increased to above 1.0 ML, we observed remarkable changes.

Figures 1(c)–(f) show STM images of Si(111) surfaces with Mg coverages of 1.0 (c), 2.0 (d), 4.0 (e), and 6.0 ML (f). At a coverage of 1.0 ML (figure 1(c)), the Si(111)-7 × 7 surface is fully covered by the deposited Mg overlayer that seems to be comprised of amorphous Mg. The amorphous nature of this overlayer was confirmed by the diffuse 7 × 7 ($\delta 7 \times 7$) LEED pattern observed for this system (see figure 4(b)). The tendency of the adsorbed Mg atoms to form a disordered overlayer rather than a well-ordered structure can be attributed to the large lattice mismatch between the a-axis of hexagonal Mg (3.21 Å) [14] and Si(111) (3.84 Å). It has been reported that Mg atoms generally react with surface Si atoms to form Mg silicide with the stoichiometry of Mg_2Si even at RT [9–11]. Hence, we expect that the disordered domains observed in figure 1(c) represent an initial stage during the formation of a Mg silicide overlayer on the Si(111) 7 × 7 surface. At this coverage, small grains of Mg clusters react with the substrate to form Mg silicide. These grains can then act as nucleation seeds upon further Mg deposition on the surface.

As the deposition of Mg atoms is increased beyond 1.0 ML, we can clearly discern the growth mode. Figure 1(d) shows an empty-state STM image of the Mg-adsorbed Si(111) surface at a coverage of 2.0 ML Mg. As shown in this image, small-sized Mg islands (3–6 nm) begin to form, which can then act as nucleation sites. Given that these Mg island domains are somewhat amorphous, we can exclude the formation of $\frac{2}{3}\sqrt{3}$ (ordered) silicide regions. Concurrently, we confirmed that a $(1 \times 1)_{Mg}$ LEED pattern is observed at this coverage. We can distinguish the (1 × 1) LEED spots of Mg ($(1 \times 1)_{Mg}$) from those of Si ($(1 \times 1)_{Si}$) due to the different lattice constant (see figures 4(a) and (d)). Our interpretation of the STM images is that the observed several-nanometre-sized Mg clusters formed by agglomeration of incident Mg atoms are simply located on the amorphous Mg silicide layers shown in figure 1(c). The 1 h time interval between the STM measurements of figures 1(c) and (d) may be sufficient for the stabilization of amorphous Mg silicide layers shown in figure 1(c). Amorphous Mg silicide layers can be stabilized by the surface diffusion induced Mg clusters followed by the formation of nucleation sites for additional clustering on them. This process would prevent the incoming Mg atoms from easily reacting with the Mg silicide layers, causing these atoms to cluster with

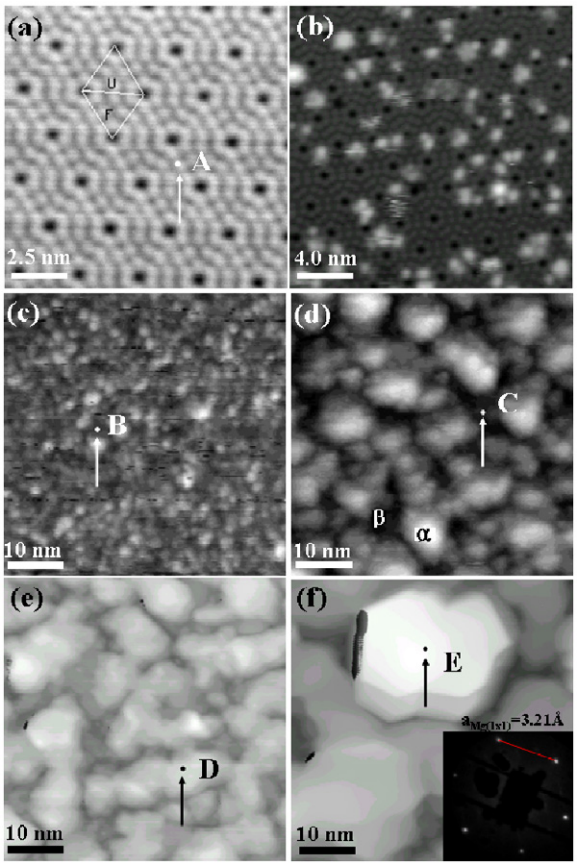

Figure 1. Empty-state STM images of Mg adsorbed on a Si(111) surface at various coverages (multi-step deposition, $V_s = 2.0$ V, 0.1 nA). (a) Clean Si(111)-7 × 7 (image size: 12.5 nm × 12.5 nm), (b) 0.1 ML Mg adsorbed on Si(111)-7 × 7 (20 nm × 20 nm), (c) amorphous Mg silicide overlayer formed on the Si(111) 7 × 7 surface (1.0 ML). Small Mg grains are observed that can act as nucleation sites upon further Mg deposition (50 nm × 50 nm), (d) Mg clustering to form Mg islands (2.0 ML, 50 nm × 50 nm), (e) overlayers of larger-sized Mg clusters on the amorphous Mg silicide layers (4.0 ML, 50 nm × 50 nm), and (f) round-shaped Mg islands grown on the Mg silicide layers (6.0 ML, 50 nm × 50 nm). These STM images were taken at intervals of 1 h. The inset of figure 2(f) displays $(1 \times 1)_{Mg}$ LEED pattern.

each other rather than react with the amorphous Mg silicide layer. As we will discuss below, the preferential clustering is also related to the surface diffusion of Mg atoms. Close inspection of figure 1(d) clearly reveals bright spots where the Mg clusters (labelled $\boldsymbol{\alpha}$) form overlayers on the Mg silicide regions (e.g., dark region labelled $\boldsymbol{\beta}$).

The STM image recorded at a coverage of 4.0 ML (figure 1(e)) differs markedly from those recorded at lower coverage. Specifically, the Mg clusters increase in size and the two different phases observed at a coverage of 2.0 ML (figure 1(d)) disappear. However, regions of ordered Mg silicide are still not observed, even at this coverage. The lack of ordered Mg silicide can be explained by the observation that the surface corrugations observed in figure 1(d) have mostly disappeared, and hence the system starts to form Mg overlayers on the amorphous (stabilized) Mg silicide layers. Such Mg overlayers without crystalline (hexagonal) structure are due to the pseudomorphic growth on the amorphous Mg silicide layers.

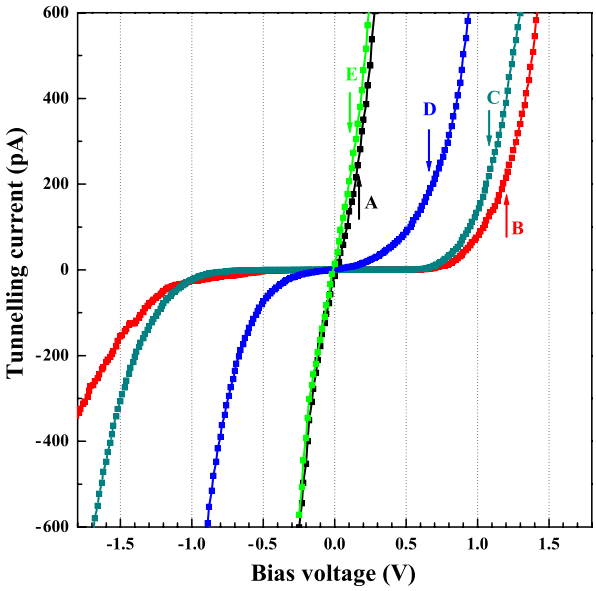

Figure 2. Tunnelling current as a function of bias voltage from STS at various Mg coverages (following the Mg coverages shown in figure 1). At very high Mg coverage (as high as 6.0 ML), the large stiffness curve (marked as E) indicates the formation of a metallic Mg film.

When the Mg coverage was further increased to 6.0 ML, we found that round Mg islands formed on the amorphous Mg silicide layers (figure 1(f)). The average size of these islands was estimated to be about 20 nm. Moreover, we found that when we further increased the Mg coverage, the average size of the Mg islands remained constant at ∼20 nm, with the height of the islands increasing with increasing coverage. This indicates that 6.0 ML represents a critical coverage beyond which the Mg island size does not change. For all Mg coverages above 2.0 ML, $(1 \times 1)_{\mathrm{Mg}}$ LEED patterns were observed (inset of figure 1(f)). Because most substrate is covered with a Mg island, the LEED pattern corresponds to the on-top structure of Mg islands. Hence, the STM and LEED results strongly suggest that no ordered array forms in the overlayer during this growth process (multi-step Mg deposition).

To confirm the electronic properties as a function of Mg coverage, we recorded STS I–V curves under the same tunnelling condition (at varying bias voltage between -1.8 and 1.8 V) at coverages corresponding to the STM images in figure 1. These I–V curves, shown in figure 1, were taken from the marked point in each STM image (the white or black dot is the area in which we conducted STS measurements). The I–V curves show a clear discrepancy with varying the Mg coverage. The spectrum of the clean Si(111)-7 × 7 surface (marked as A) shows no apparent band gap, which is consistent with the metallic property of the Si(111)-7 × 7 surface. At Mg coverages of 1.0 and 2.0 ML (marked as B and C), however, we found band gaps indicative of the semiconducting Mg silicide. On increasing the Mg coverage to 4.0 ML (marked as D), we observed a decrease in the band gap consistent with metallization. Interestingly, the film deposited at 6.0 ML Mg (marked as E) shows no apparent gap, indicating metallic behaviour. The STS results thus demonstrate that a metallic Mg overlayer dominates for coverages above 4.0 ML.

To see the morphological changes for the single-step process, we deposited Mg on Si(111)-7 × 7 up to 4.0 ML or 10.0 ML at RT. Figure 3(a) shows an STM image of the surface after

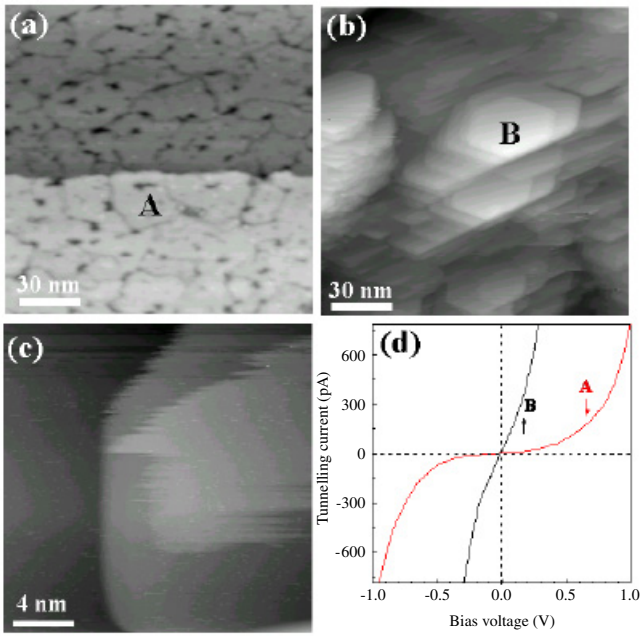

Figure 3. Empty-state STM images of Mg-adsorbed Si(111) surfaces at two coverages (single-step deposition). (a) Broad and flat areas due to the formation of Mg_2Si silicide begin to appear. This plateau has a $\frac{2}{3}\sqrt{3}$ LEED pattern (4.0 ML, $V_s = 2.0$ V, 150 nm $\times$ 150 nm). (b) Thick Mg film grown on the Si(111) surface comprised of hexagonally close-packed layers of Mg atoms (10.0 ML, $V_s = 2.0$ V, 100 nm $\times$ 100 nm). (c) Low bias voltage image, indicating metallic properties of islands ($V_s = 10$ mV, 20 nm $\times$ 20 nm). (d) STS I–V curves for the two coverages shown in (a) and (b).

4.0 ML Mg deposition via the single-step process. This image shows a broad and flat area typical of the formation of Mg silicide. Inspection of the STS I–V curve for this system (marked **A** in figure 3(a)) reveals a broad voltage–current gap, indicating that this surface is semiconducting. Moreover, it has been reported that Mg_2Si is the only stoichiometric phase of Mg silicide with a direct band gap of 2.17 eV and an indirect band gap of 0.6–0.8 eV range [15]. Our STS data thus indicate that the adsorbed Mg atoms react with the Si substrate atoms to form a well-ordered semiconducting Mg silicide layer, even at RT. Consistent with this, we found using LEED analysis that this surface showed well-ordered $\frac{2}{3}\sqrt{3}$ periodicity (see figure 4(c)), in agreement with previous results [9, 10].

When the coverage of Mg deposited by the single-step process was increased to 10.0 ML, thick Mg islands with hexagonal shapes were formed (figure 3(b)). These hexagonal Mg islands were shown to be a mixed phase of $\frac{2}{3}\sqrt{3}$ and 1×1 periodicity, as confirmed by LEED analysis (see figure 4(d)). The STM image clearly shows that, at this coverage, the Mg atoms are hexagonally packed on the flat Mg silicide surface (figure 3(a)). Bulk crystalline Mg has a hexagonal-close-packed (hcp) structure with lattice constants of 3.21 Å (axis a) and 5.21 Å (axis c), respectively [14]. In our STM image, we can see the stack of hexagonally packed layers that comprise each hexagonally shaped Mg island. From the shape of the Mg islands, we can strongly infer that the islands are formed from the stacking of the Mg atoms in a manner analogous to the bulk crystallization of Mg. Our observation of a $(1 \times 1)_{Mg}$ LEED pattern indicates the formation of Mg islands on the Mg_2Si overlayer, which gives rise to a $\frac{2}{3}\sqrt{3}$ LEED pattern. Figure 3(c) shows an empty-state STM image obtained from the edges of a Mg

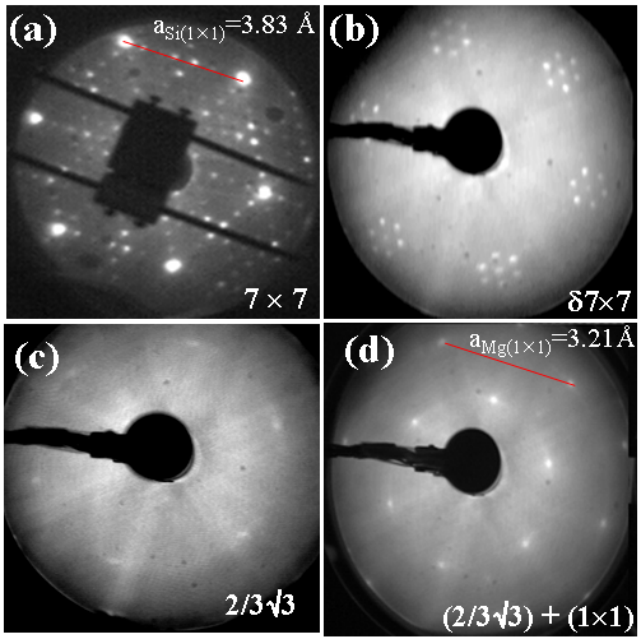

Figure 4. Representative LEED patterns observed at various Mg coverages by continuous Mg deposition (a) 7×7 (clean) (b) diffuse 7×7 ($\delta 7 \times 7$, 0.1 ML), (c) $\frac{2}{3}\sqrt{3}$ (4.0 ML), (d) mixed $\frac{2}{3}\sqrt{3}$ and $(1 \times 1)_{Mg}$ pattern (10.0 ML).

island at low bias voltage ($V_s = 10$ mV) shown in figure 3(b). STS data also strongly support the metallic nature of these islands. Specifically, the STS curve (marked as **B** in figure 3(d)) do not show a gap indicative of semiconducting properties. Hence, this is strong evidence of the growth of metallic Mg islands.

Our results for single-step Mg deposition indicate that the Mg island initially forms on the flat Mg_2Si overlayer with $\frac{2}{3}\sqrt{3}$ ordered periodicity, and that the height of this island becomes large while the island size remains nearly unchanged during further Mg deposition. We can therefore conclude that the growth of the Mg film follows a Stranski–Krastanov (SK)-like mode.

Figure 4 shows the LEED patterns for the Si(111)-7×7 surface with various Mg coverages by continuous Mg deposition. As the Mg coverage increases, the (a) 7×7 LEED pattern gradually weakens and (b) diffuse 7×7 ($\delta 7 \times 7$), (c) $\frac{2}{3}\sqrt{3}$ and (d) mixed $\frac{2}{3}\sqrt{3}$ and $(1 \times 1)_{Mg}$ LEED patterns successively appear.

The two different growth processes of Mg islands (single-step and multi-step deposition) are depicted schematically in figure 5. When the Mg is deposited stepwise, with the coverage being increased at 1 h time intervals (multi-step deposition), flat Mg islands with a hexagonal structure cannot form. Rather, under these deposition conditions, individual Mg clusters on the amorphous Mg silicide overlayer act as nucleation sites for the formation and growth of round-shaped Mg islands. The adsorbed Mg atoms settle on their energetically most favourable sites on the Si(111) surface shortly after impinging on the amorphous Mg silicide surface, leading to the formation of amorphous Mg silicide layers with larger grains. When additional Mg atoms are subsequently deposited after a certain time interval (1 h in our experiments), the new incoming Mg atoms meet with a substrate comprised of an amorphous Mg silicide layer on which already adsorbed Mg atoms are arranged as dimers, trimers, and higher clusters. As

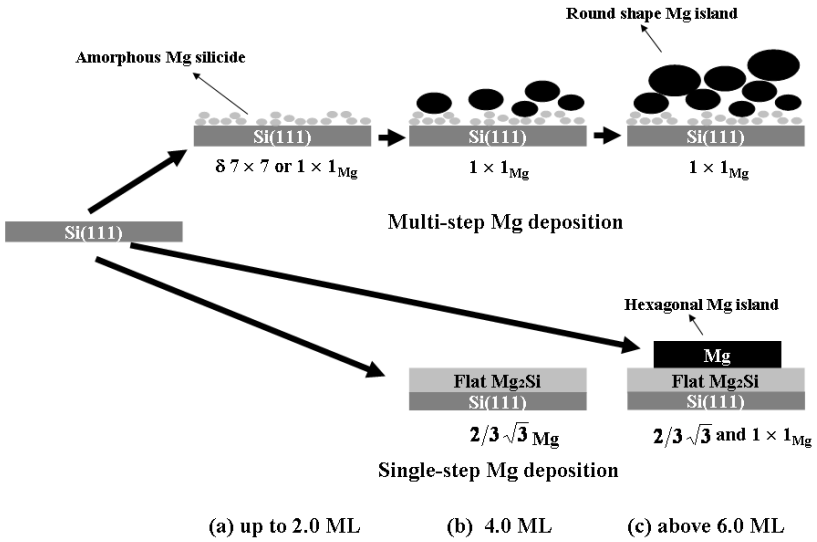

Figure 5. Schematic diagrams depicting the process of Mg island formation at various coverages according to an SK-like growth mode. The diagrams show how the two different processes of Mg deposition on the Si(111) surface give rise to Mg islands with very different morphologies.

the number of Mg atoms in a cluster increases, the cluster size gradually increases to form a round-shaped Mg island.

In contrast to the behaviour during multi-step deposition, continuous Mg deposition (single-step deposition) leads to the formation of Mg islands with a hexagonal structure on the flat Mg_2Si overlayer. When the Mg coverage exceeds the value required for Mg silicide formation (4.0 ML in our system), ordered Mg_2Si layers with a $\frac{2}{3}\sqrt{3}$ structure grow pseudomorphically due to relaxed lattice mismatches between the Si and Mg silicide. Upon further Mg deposition (above 6.0 ML), hexagonal Mg islands grow on the Mg_2Si layers. These islands are comprised of hexagonally packed layers; thus their structure is the same as the bulk hcp structure. The Mg island growth follows the SK mode, as strongly supported by the mixed $\frac{2}{3}\sqrt{3}$ and $(1 \times 1)_{Mg}$ LEED pattern (figure 4(d)) and the band-gap change in the STS I–V curve. The growth of hexagonal Mg islands can be primarily attributed to pseudomorphic growth on the Si(111) substrate covered by a flat Mg_2Si overlayer (see figure 3). This flat layer forms a diffusion barrier so no incoming Mg can reach the flat Mg_2Si overlayer any more; hence additionally deposited Mg forms hexagonal islands of metallic Mg with the hcp structure of bulk crystalline Mg.

The difference between the two growth modes can be explained by the surface kinetic and thermodynamic considerations. We ignore the latter because of the same substrate temperature between two types of Mg growth. Hence, we only focus on the former. Although there are several factors which govern the surface kinetics, the main difference is the Mg deposition flux, which will affect the surface diffusion. There is an explicit relation between deposition flux and mean free diffusion path of single adatoms deposited on the substrate. It can be briefly represented as $l \approx (D/F)^{1/6}$ where l is the mean free path of diffusing adatoms, D is the intrinsic diffusion coefficient and F is the deposition flux [16]. In our experimental case, D is constant due to the same kind of adatoms (Mg). Therefore we can use this relation just comparing with different values of F between the two types of Mg deposition. Because the

F of multi-step deposition is lower than that of single-step deposition, we can judge from the above relation that there should be higher l upon multi-step Mg deposition compared with single-step case. In [16], l is defined as a characteristic length which is directly related to the mean free path of diffusing adatoms before they create a new nucleation site or are captured by an existing island. Considering this logic, we can at least suggest that Mg adatoms from multi-step deposition easily diffuse to cluster with existing nucleation sites (the clusters in figure 1(b), for example). As the Mg coverage is increased, incoming adatoms also diffuse to clusters in the same manner. As a consequence, the island (Volmer–Wever) growth mode dominates the overall Mg growth in multi-step Mg deposition. With single-step Mg deposition, on the other hand, a flat Mg_2Si layer with $\frac{2}{3}\sqrt{3}$ periodicity on the Si(111)-7 $\times$ 7 surface is formed due to limited adatom diffusion on the substrate. The incoming Mg adatoms would directly react with Si atoms on the substrate rather than diffuse to cluster with each other. Therefore they form a flat Mg_2Si layer, followed by pseudomorphic hexagonal Mg growth on the flat Mg_2Si layer (SK-like growth).

4. Conclusions

We have shown that the mechanism by which Mg islands grow on a Si(111)-7 $\times$ 7 surface, and the morphology of the islands formed, depends on whether the Mg deposition is performed in a stepwise or continuous manner. When the Mg atoms were deposited in multiple steps, with 1 h between deposition events, an amorphous Mg silicide layer was formed during the initial stage of Mg coverage (up to 2.0 ML) due to the lattice mismatch between the Si and Mg atoms. As the stepwise Mg deposition proceeded to coverages above 6.0 ML, round-shaped Mg islands with a critical island size of 20 nm were formed on the amorphous Mg silicide layers over the Si(111)-7 $\times$ 7 surface. If, on the other hand, the Mg was deposited continuously in a single step, hexagon-shaped Mg islands formed via a broad and flat Mg_2Si layer with $\frac{2}{3}\sqrt{3}$ periodicity on the Si(111)-7 $\times$ 7 surface, following an SK-like growth mode. Measurements of STS I–V curves confirmed the metallic and semiconducting properties of the Mg islands and silicide layers, respectively.

Acknowledgments

This work was supported by the Korea Science and Engineering Foundation (KOSEF) grant funded by the Korea government (MOST) (No. R01-2006-000-11247-0), and one of authors (Professor Sehun Kim) was also supported by the Brain Korea 21 project, the SRC program (Center for Nanotubes and Nanostructured Composites) of MOST/KOSEF, the National R&D Project for Nano Science and Technology, and Korea Research Foundation Grant No. KRF-2005-070-C00063.

References

[1] Freeouf J L 1983 *Surf. Sci.* **132** 233
[2] Mönch W 1990 *Rep. Prog. Phys.* **53** 221
[3] Kang M-H, Kang J-H and Jeong S 1998 *Phys. Rev.* B **58** R13359
[4] Lee G, Hong S, Kim H, Shin D, Koo J-Y, Lee H-I and Moon D W 2001 *Phys. Rev. Lett.* **87** 056104
[5] Benemanskaya G V, Daineka D V and Frank-Kamenetskaya G E 1999 *J. Phys.: Condens. Matter* **11** 6679
[6] Shi H Q, Radny M W and Smith P V 2004 *Phys. Rev.* B **70** 235325
[7] Miwa R H 2005 *Phys. Rev.* B **72** 085325
[8] Vandre D, Incoccia L and Kaindl G 1990 *Surf. Sci.* **225** 233
[9] Quinn J and Jona F 1991 *Surf. Sci. Lett.* **249** L307

[10] Wirgen C, Andersen J N, Nyholm R and Karlsson U O 1993 *Surf. Sci.* **289** 290
[11] An K S, Park R J, Kim J S, Park C Y, Kim C Y, Chung J W, Abukswa T, Kono S, Kinoshita T, Kakizaki A and Ishii T 1995 *Surf. Sci. Lett.* **337** 789
[12] An K S, Park R J, Kim J S, Park C Y, Lee S B, Abukswa T, Kono S, Kinoshita T, Kakizaki A and Ishii T 1995 *J. Appl. Phys.* **78** 1151
[13] Kubo O, Saranin A A, Zotov A V, Ryu J-T, Tani H, Harada T, Katayama M, Lifshits V G and Oura K 1998 *Surf. Sci.* **415** L971
[14] Lide D R (ed) 1998 *CRC Handbook of Chemistry and Physics* 79th edn (Boca Raton, FL: CRC Press) section 12-10
[15] Wyckoff R W G 1963 *Crystal Structures* vol 1 (New York: Interscience)
[16] Brune H 1998 *Surf. Sci. Rep.* **31** 125